

# $J/\psi$ and $D^*$ Mesons Photoproduction at HERA

V.A.Saleev<sup>1,2</sup> and D.V.Vasin<sup>1</sup>

<sup>1</sup> Samara State University, Samara, 443011, Russia

<sup>2</sup> Samara Municipal Nayanova University, Samara, 443001, Russia

**Abstract.** In this report we compare the predictions of the collinear parton model and the  $k_T$ -factorization approach in  $J/\psi$  and  $D^*$  meson photoproduction at HERA energies. It is shown that obtained  $D^*$  meson spectra over  $p_T$  and  $\eta$  are very similar in the parton model and  $k_T$ -factorization approach and they underestimate the experimental data. Opposite, the predictions of the both approaches for  $p_T$ - and  $z$ -spectra in the  $J/\psi$  photoproduction are very different as well as the prediction obtained for the spin parameter  $\alpha(p_T)$ .

## 1 Hard Processes in the Parton Model and $k_T$ -Factorization Approach

Nowadays, there are two approaches which are used in a study of the charmonia and charmed mesons photoproduction at high energies. In the conventional collinear parton model [1] it is suggested that hadronic cross section, for example  $\sigma(\gamma p \rightarrow c\bar{c}X, s)$ , and the relevant partonic cross section  $\hat{\sigma}(\gamma g \rightarrow c\bar{c}, \hat{s})$  are connected as follows

$$\sigma^{PM}(\gamma p \rightarrow c\bar{c}X, s) = \int dx G(x, \mu^2) \hat{\sigma}(\gamma g \rightarrow c\bar{c}, \hat{s}), \quad (1)$$

where  $\hat{s} = xs$ ,  $G(x, \mu^2)$  is the collinear gluon distribution function in a proton,  $x$  is the fraction of a proton momentum,  $\mu^2$  is the typical scale of a hard process. The  $\mu^2$  evolution of the gluon distribution  $G(x, \mu^2)$  is described by DGLAP evolution equation [2]. In the so-called  $k_T$ -factorization approach hadronic and partonic cross sections are related by the following condition [3–5]:

$$\sigma^{SHA}(\gamma p \rightarrow cX, s) = \int \frac{dx}{x} \int dk_T^2 \int \frac{d\varphi}{2\pi} \Phi(x, k_T^2, \mu^2) \hat{\sigma}(\gamma g^* \rightarrow c\bar{c}, \hat{s}, k_T^2), \quad (2)$$

where  $\hat{\sigma}(\gamma g^* \rightarrow c\bar{c}, \hat{s}, k_T^2)$  is the  $c\bar{c}$ -pair photoproduction cross section on off mass-shell gluon,  $k^2 = k_T^2 = -k_T^2$  is the gluon virtuality,  $\hat{s} = xs - k_T^2$ ,  $\varphi$  is the azimuthal angle in the transverse XOY plane between vector  $k_T$  and the fixed OX axis. The unintegrated gluon distribution function  $\Phi(x, k_T^2, \mu^2)$  can be related to the conventional gluon distribution by

$$xG(x, \mu^2) = \int_0^{\mu^2} \Phi(x, k_T^2, \mu^2) dk_T^2, \quad (3)$$

where  $\Phi(x, \mathbf{k}_T^2, \mu^2)$  satisfies the BFKL evolution equation [6]. In formulae (2) the four-vector of a gluon momentum is presented as follows:

$$k = xp_N + k_T, \quad (4)$$

where  $k_T = (0, \mathbf{k}_T, 0)$ ,  $p_N = (E_N, 0, 0, E_N)$  is the four-vector of a proton momentum. At the  $x \ll 1$  the off mass-shell gluon has dominant longitudinal polarization along the proton momentum. Taking into account the gauge invariance of a total amplitude involving virtual gluon we can write the polarization four-vector in two different forms:

$$\varepsilon^\mu(k) = \frac{k_T^\mu}{|\mathbf{k}_T|} \quad (5)$$

or

$$\varepsilon^\mu(k) = -\frac{xp_N^\mu}{|\mathbf{k}_T|}. \quad (6)$$

As it will be shown above formulae (5) and (6) give the equal answers in calculating of squared amplitudes under consideration.

Our calculation in the parton model is done using the GRV LO [7] parameterization for the collinear gluon distribution function  $G(x, \mu^2)$ . In the case of the  $k_T$ -factorization approach we use the following parameterizations for an unintegrated gluon distribution function  $\Phi(x, \mathbf{k}_T^2, \mu^2)$ : JB by J. Bluemlein [8]; JS by H. Jung and G. Salam [9]; KMR by M.A. Kimber, A.D. Martin and M.G. Ryskin [10]. The detail analysis of the evolution equations lied in a basis of the different parameterizations is over our consideration. To compare different parameterizations we have plotted their as a function of  $x$  at the fixed  $\mathbf{k}_T^2$  and  $\mu^2$  in Fig. 1 and as a function of  $\mathbf{k}_T^2$  at the fixed  $x$  and  $\mu^2$  in Fig. 2.

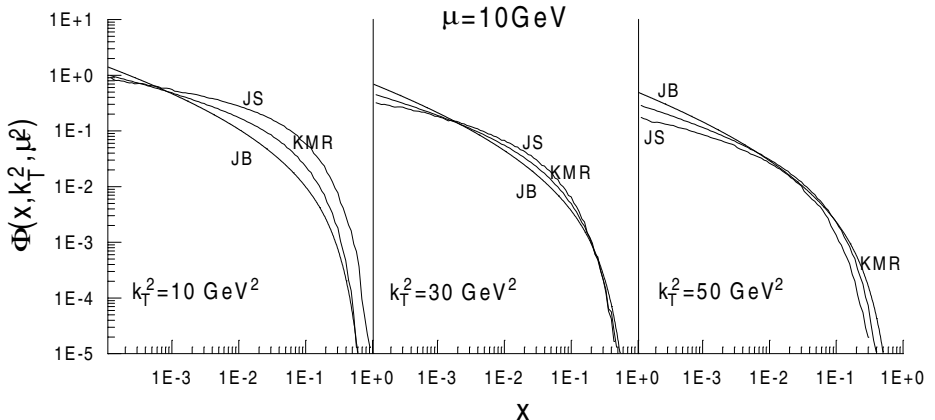


**Fig. 1.** The unintegrated gluon distribution function  $\Phi(x, \mathbf{k}_T^2, \mu^2)$  versus  $x$  at the fixed values of  $\mu$  and  $\mathbf{k}_T^2$ .

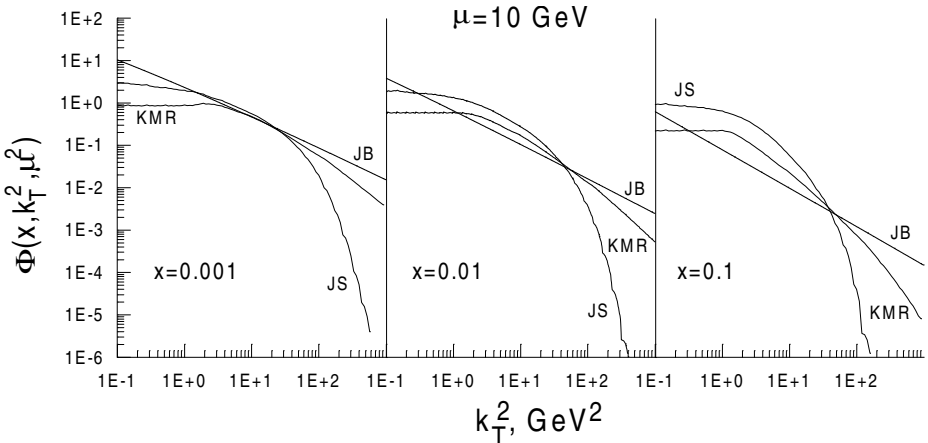


**Fig. 2.** The unintegrated gluon distribution function  $\Phi(x, k_T^2, \mu^2)$  versus  $k_T^2$  at the fixed values of  $\mu$  and  $x$ .

Note, that all parameterizations of an unintegrated gluon distribution function describe the data from HERA collider for the structure function  $F_2(x, Q^2)$  well [8–10].

## 2 $D^*$ Meson Photoproduction in LO QCD

The photoproduction of the  $D^*$  meson was studied experimentally by H1 and ZEUS collaborations at HERA ep-collider ( $E_e = 27.5$  GeV,  $E_N = 820$  GeV) [11,12]. Because of the large mass of a  $c$ -quark usually it is assumed that  $D^*$  meson production may be described in the fragmentation approach<sup>1</sup> [13], where

$$\sigma(\gamma p \rightarrow D^* X, p) = \int D_{c \rightarrow D^*}(z, \mu^2) \sigma(\gamma p \rightarrow cX, p_1 = p/z) dz \quad (7)$$

and  $D_{c \rightarrow D^*}(z, \mu^2)$  is the universal fragmentation function of a  $c$ -quark into the  $D^*$  meson at the scale  $\mu^2 = m_D^2 + p_T^2$ . The fraction of the  $D^*$  produced by a  $c$ -quark as measured by OPAL Collaboration [15],

$$\omega_{c \rightarrow D^*} = \int_0^1 D_{c \rightarrow D^*}(z, \mu^2) dz = 0.222 \pm 0.014,$$

has been used in our LO QCD calculations to normalize the fragmentation function.

<sup>1</sup> The another approach based on recombination scenario was suggested recently in [14]

The Peterson [13] fragmentation function was used as a phenomenological factor:

$$D_{c \rightarrow D^*}(z, \mu_0^2) = N \frac{z(1-z)^2}{[(1-z)^2 + \epsilon z]^2}. \quad (8)$$

In the high energy limit or in the case of a massless quark one has following relation for the four-vectors  $p = zp_1$ , however in the discussed here process the  $D^*$  meson energy is not so large in compare to  $M_{D^*}$  and the following prescription was used

$$\mathbf{p} = z\mathbf{p}_1 \quad (9)$$

together with the mass-shell condition for the  $c$ -quark energy and momentum  $E_1^2 = \mathbf{p}_1^2 + m_c^2$ . We have used  $\epsilon = 0.06$  as a middle value between two recent fits of  $D^*$  meson spectra in  $e^+e^-$ -annihilation, which based on massive charm ( $\epsilon = 0.036$ )[16] and massless charm ( $\epsilon = 0.116$ )[17] calculations. The squared matrix element for the subprocess  $\gamma g^* \rightarrow c\bar{c}$  after summation over a gluon polarization accordingly (6) may be written as follows [4,5,18]:

$$|M|^2 = 16\pi^2 e_c^2 \alpha_s \alpha \cdot (\hat{s} + \mathbf{k}_T^2)^2 \left[ \frac{\alpha_1^2 + \alpha_2^2}{(\hat{t} - m_c^2)(\hat{u} - m_c^2)} - \frac{2m_c^2}{\mathbf{k}_T^2} \left( \frac{\alpha_1}{\hat{u} - m_c^2} - \frac{\alpha_2}{\hat{t} - m_c^2} \right)^2 \right] \quad (10)$$

where  $\hat{s}$ ,  $\hat{t}$  and  $\hat{u}$  are usual Mandelstam variables,

$$\alpha_1 = \frac{m_c^2 + \mathbf{p}_{1T}^2}{m_c^2 - \hat{t}}, \quad \alpha_2 = \frac{m_c^2 + \mathbf{p}_{2T}^2}{m_c^2 - \hat{u}},$$

$\mathbf{p}_{1T}$  and  $\mathbf{p}_{2T}$  are the transverse momenta of  $c$ - and  $\bar{c}$ -quarks,  $\mathbf{k}_T = \mathbf{p}_{1T} + \mathbf{p}_{2T}$ .

Using formulas (5) for a BFKL gluon polarization four-vector we can rewrite (10) in the another form:

$$\begin{aligned} \overline{|M|^2} = & \frac{16\pi^2 e_c^2 \alpha_s \alpha}{(m_c^2 - \hat{t})^2 (m_c^2 - \hat{u})^2} \left[ m_c^2 \left( -2m_c^6 - 4m_c^2 \mathbf{p}_{1T}^2 \mathbf{k}_T^2 + m_c^2 \mathbf{k}_T^4 + 8\mathbf{p}_{1T}^2 \mathbf{k}_T^4 + \right. \right. \\ & + 3\mathbf{k}_T^6 + (4m_c^4 + 12\mathbf{p}_{1T}^2 \mathbf{k}_T^2 + 5\mathbf{k}_T^4) \hat{s} - (3m_c^2 - 4\mathbf{p}_{1T}^2 - 3\mathbf{k}_T^2) \hat{s}^2 + \hat{s}^3 \Big) + \\ & + \left( 8m_c^6 + 8m_c^2 \mathbf{p}_{1T}^2 \mathbf{k}_T^2 - 2m_c^2 \mathbf{k}_T^4 - 4\mathbf{p}_{1T}^2 \mathbf{k}_T^4 - \mathbf{k}_T^6 - 12m_c^4 \hat{s} - 4\mathbf{p}_{1T}^2 \mathbf{k}_T^2 \hat{s} - \right. \\ & - \mathbf{k}_T^4 \hat{s} + 6m_c^2 \hat{s}^2 - \mathbf{k}_T^2 \hat{s}^2 - \hat{s}^3 \Big) \hat{t} - \left( 4\mathbf{p}_{1T}^2 \mathbf{k}_T^2 - \mathbf{k}_T^4 + 3(-2m_c^2 + \hat{s})^2 \right) \hat{t}^2 + \\ & + 4 \left( 2m_c^2 - \hat{s} \right) \hat{t}^3 - 2\hat{t}^4 - 4|\mathbf{p}_{1T}| \left( |\mathbf{k}_T| \cos(\varphi) \left( -2m_c^6 - \right. \right. \\ & - \left( \mathbf{k}_T^2 - \hat{s} - 2\hat{t} \right) \hat{t} \left( 2m_c^2 - \hat{u} \right) + m_c^4 \left( \mathbf{k}_T^2 + 3\hat{s} + 6\hat{t} \right) + m_c^2 \left( 3\mathbf{k}_T^4 + \hat{s}^2 + \right. \right. \\ & + \mathbf{k}_T^2 (4\hat{s} - 2\hat{t}) - 6\hat{s}\hat{t} - 6\hat{t}^2 \Big) \Big) + |\mathbf{p}_{1T}| \cos(2\varphi) \left( m_c^4 \mathbf{k}_T^2 + \mathbf{k}_T^2 \hat{t} \left( 2m_c^2 - \hat{u} \right) - \right. \\ & \left. \left. - m_c^2 \left( 2\mathbf{k}_T^4 + \hat{s}^2 + \mathbf{k}_T^2 (3\hat{s} + 2\hat{t}) \right) \right) \right) \Big], \end{aligned} \quad (11)$$

where  $\varphi$  is the angle between  $\mathbf{p}_{1T}$  and  $\mathbf{k}_T$ .

In the last case (11) it is easy to find the parton model limit:

$$\lim_{|\mathbf{k}_T| \rightarrow 0} \int_0^{2\pi} \frac{d\varphi}{2\pi} \overline{|M|^2} = \overline{|M_{PM}|^2}, \quad (12)$$

where

$$\mathbf{p}_{1T}^2 = \mathbf{p}_{2T}^2 = \frac{(\hat{u} - m_c^2)(\hat{t} - m_c^2)}{\hat{s}} - m_c^2,$$

and

$$\begin{aligned} \overline{|M_{PM}|^2} = & -\frac{16\pi^2 e_c^2 \alpha_s \alpha}{(9(m_c^2 - \hat{t})^2(-m_c^2 + \hat{s} + \hat{t})^2)} \left[ -2m_c^8 + 8m_c^6(\hat{s} + \hat{t}) - \right. \\ & -\hat{t}(\hat{s}^3 + 3\hat{s}^2\hat{t} + 4\hat{s}\hat{t}^2 + 2\hat{t}^3) + m_c^2(\hat{s}^3 + 6\hat{s}^2\hat{t} + 8\hat{t}^3 + 4\hat{s}\hat{t}(3\hat{t} + \hat{u})) - \\ & \left. -m_c^4(7\hat{s}^2 + 12\hat{t}^2 + 4\hat{s}(4\hat{t} + \hat{u})) \right] \end{aligned} \quad (13)$$

### 3 $D^*$ Meson Photoproduction at HERA

In this part we will compare our results obtained with leading order matrix elements for the partonic subprocess  $\gamma g \rightarrow c\bar{c}$  in the conventional parton model as well as in the  $k_T$ -factorization approach with data from HERA ep-collider. The data under consideration taken by the ZEUS Collaboration [11]. Inclusive photoproduction of the  $D^{*\pm}$  mesons has been measured for the photon-proton center-of-mass energies in the range  $130 < W < 280$  GeV and the photon virtuality  $Q^2 < 1$  GeV $^2$ . At low  $Q^2$  the cross section for  $ep \rightarrow eD^*X$  are related to  $\gamma p$  cross section using the equivalent photon approximation [19]:

$$d\sigma_{ep} = \int \sigma_{\gamma p} \cdot f_{\gamma/e}(y) dy,$$

where  $f_{\gamma/e}(y)$  denotes the photon flux integrated over  $Q^2$  from the kinematic limit of  $Q_{min}^2 = m_e^2 y^2 / (1 - y)$  to the upper limit  $Q_{max}^2 = 1$  GeV $^2$ ,  $y = W^2/s$ ,  $s = 4E_N E_e$ ,  $E_N$  and  $E_e$  are the proton and electron energies in the laboratory frame.

The exact formulas for  $f_{\gamma/e}(y)$  is taken from [20]:

$$f_{\gamma/e}(y) = \frac{\alpha}{2\pi} \left[ \frac{1 + (1 - y)^2}{y} \log \frac{Q_{max}^2}{Q_{min}^2} + 2m_e^2 y \left( \frac{1}{Q_{min}^2} - \frac{1}{Q_{max}^2} \right) \right].$$

The limits of integration over  $y$  are  $y_{min}^{max} = W_{min}^2 / s$ . In our calculations we used formulas for differential cross section in the following form:

$$\begin{aligned} \frac{d\sigma(ep \rightarrow eD^*X)}{d\eta dp_T} = & \int dy f_{\gamma/e}(y) \int \frac{dz}{z} D_{c \rightarrow D^*}(z, \mu^2) \int \frac{d\varphi}{2\pi} \int d\mathbf{k}_T^2 \frac{\Phi(x, \mathbf{k}_T^2, \mu^2)}{x} \times \\ & \times \frac{2|\mathbf{p}_1| |\mathbf{p}_{1T}|}{E_1(2E_N(E_1 - p_{1z}) - W^2)} \cdot \frac{|\bar{M}|^2}{16\pi x W^2} \end{aligned} \quad (14)$$

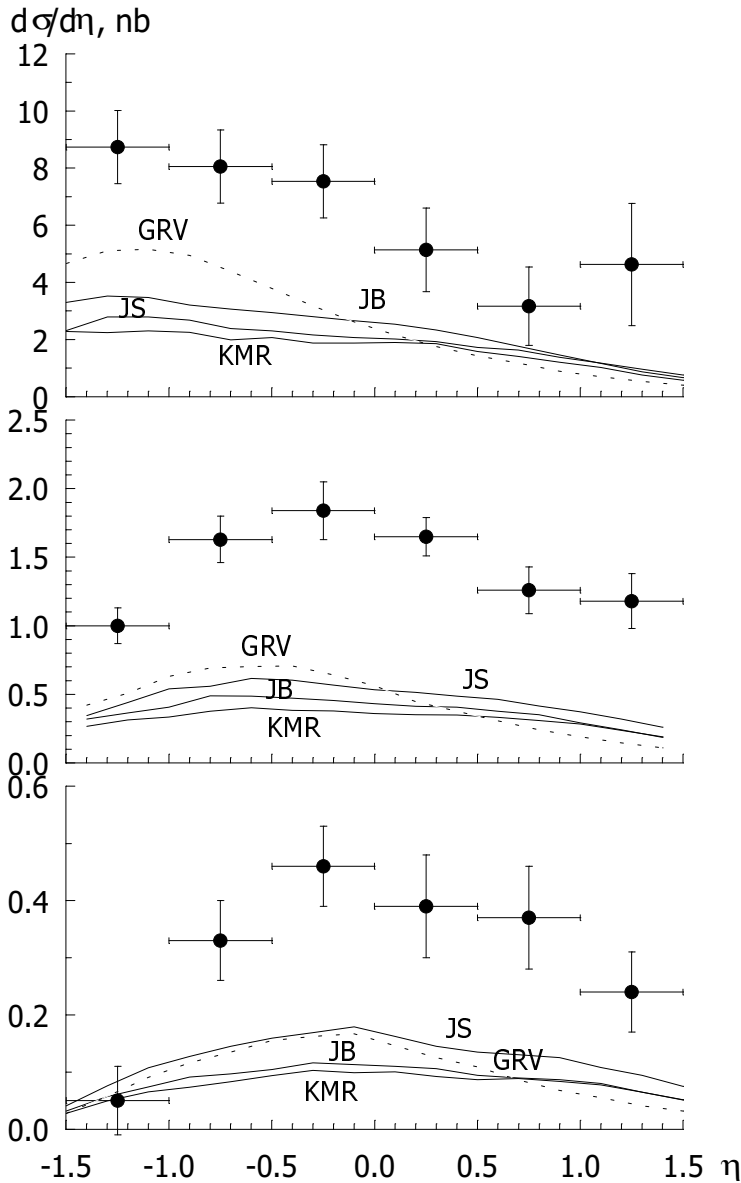


**Fig. 3.** The  $\eta$  spectra of the  $D^*$  meson at the various cut on a transverse momentum ( $p_T > 2, 4, 6$  GeV, correspondingly from up to down) and  $130 < W < 280$  GeV.

The differential cross section as a function of the  $D^*$  pseudorapidity, which is defined as  $\eta = -\ln(\tan \frac{\theta}{2})$ , where the polar angle  $\theta$  is measured with respect to the proton beam direction, is shown in Fig. 3 where the kinematic ranges for

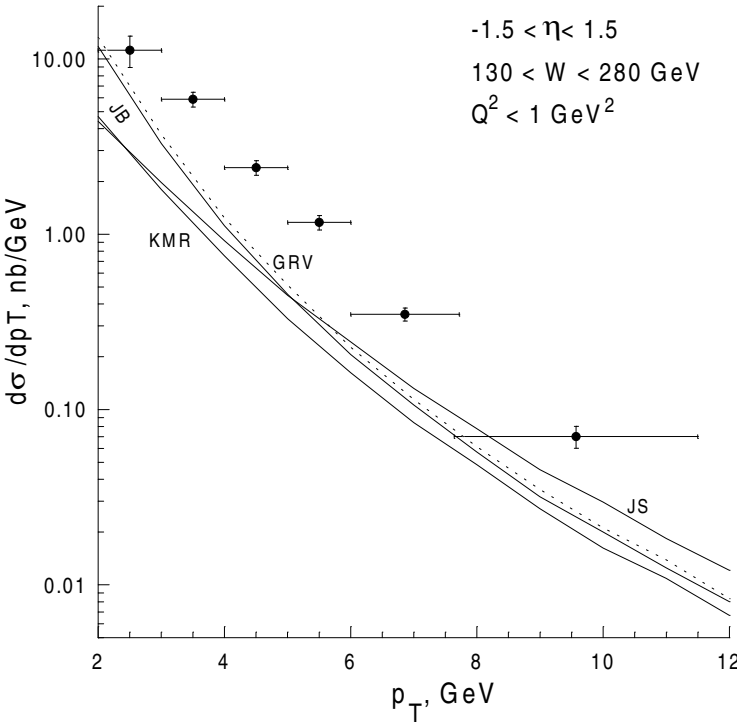


Fig. 4. The  $p_T$ -spectrum of  $D^*$  meson.

the  $D^*$  meson transverse momentum are  $2 < p_T < 12$  GeV,  $4 < p_T < 12$  GeV,  $6 < p_T < 12$  GeV, correspondingly from up to down.

We see that the results of calculations performed in the collinear parton model as well as in the  $k_T$ -factorization approach with LO in  $\alpha_s$  matrix elements need additional  $K$ -factor ( $K \approx 2$ ) to describe the data. The value of this  $K$ -factor is usual for a heavy quark production cross section in the relevant energy range. Opposite the results obtained in  $k_T$ -factorization approach with JB parameterization in [21], where the strong enhance for the cross sections at all  $\eta$  in the  $k_T$ -factorization approach in compare to the collinear parton model was demonstrated, we see only deformation of the  $\eta$ -spectra. We have obtained that at low  $p_{T\min}$  the maximum value of the cross section even higher in the collinear parton model and only at the large positive  $\eta$  the  $k_T$ -factorization approach gives more large values.

The  $p_T$  spectrum of  $D^*$  meson in photoproduction at  $|\eta| < 1.5$  and  $130 < W < 280$  GeV are shown in Fig. 4. All theoretical curves are under experimental points. As it was already mentioned typical value of the  $K$ -factor is equal 2.

Our results show that the introducing of a gluon transverse momentum  $k_T$  in the framework of the  $k_T$ -factorization approach does't increase the  $D^*$  meson photoproduction cross section at the large  $p_T$  as it is predicted for the  $J/\psi$

photoproduction [22,23] (see next part of the paper). We see the small effect in the case of JS parameterization [9] only.

The dependence of the  $D^*$  meson production cross section on a total photon-proton center-of-mass energy  $W$  is shown in Fig. 5. Nowadays the experimental data for  $d\sigma/dW$  are absent. We see that the difference between the results obtained with the various parameterizations of a unintegrated gluon distribution function is about 50%. As well in the case of the  $\eta$ -spectra. At the small  $p_{T\min}$  the cross section calculated in the parton model is larger than predictions obtained in the  $k_T$ -factorization approach.

The main uncertainties of our calculation come from the choice of a  $c$ -quark mass in the partonic matrix elements (10),(11) and (13), and from the choice of a parameter  $\epsilon$  in the Peterson fragmentation function  $D_{c\rightarrow D^*}(z, \mu^2)$ .

However, even at the very extremely choice ( $m_c \approx 1.3$  GeV and  $\epsilon \approx 0.02$ ) our theoretical predictions describe only shapes of the  $p_T$ - and  $\eta$ -spectra, but don't describe absolute values of the measured cross sections. This fact shows the famous role of the next to leading order corrections in the  $D^*$  meson photoproduction as in the parton model as in the  $k_T$ -factorization approach.

## 4 $J/\psi$ Photoproduction in LO QCD

It is well known that in the processes of  $J/\psi$  meson photoproduction on protons at high energies the photon-gluon fusion partonic subprocess dominates [24]. In the framework of the general factorization approach of QCD the  $J/\psi$  photoproduction cross section depends on the gluon distribution function in a proton, the hard amplitude of  $c\bar{c}$ -pair production as well as the mechanism of a creation colorless final state with quantum numbers of the  $J/\psi$  meson. In such a way, we suppose that the soft interactions in the initial state are described by introducing a gluon distribution function, the hard partonic amplitude is calculated using perturbative theory of QCD at order in  $\alpha_s(\mu^2)$ , where  $\mu \sim m_c$ , and the soft process of the  $c\bar{c}$ -pair transition into the  $J/\psi$  meson is described in nonrelativistic approximation using series in the small parameters  $\alpha_s$  and  $v$  (relative velocity of the quarks in the  $J/\psi$  meson). As is said in nonrelativistic QCD (NRQCD) [25], there are color singlet mechanism, in which the  $c\bar{c}$ -pair is hardly produced in the color singlet state, and color octet mechanism, in which the  $c\bar{c}$ -pair is produced in the color octet state and at a long distance it transforms into a final color singlet state in the soft process. However, as it was shown in papers [23,26], the data from the DESY ep-collider [27] in the wide region of  $p_T$  and  $z$  may be described well in the framework of the color singlet model and the color octet contribution is not needed. Based on the above mentioned result we will take into account in our analysis only the color singlet model contribution in the  $J/\psi$  meson photoproduction

[24]. We consider here the role of a proton gluon distribution function in the  $J/\psi$  photoproduction in the framework of the conventional parton model as well as in the framework of the  $k_T$ -factorization approach [3–5].

There are six Feynman diagrams (Fig. 6) which describe the partonic process  $\gamma g \rightarrow J/\psi g$  at the leading order in  $\alpha_s$  and  $\alpha$ . In the framework of the color singlet

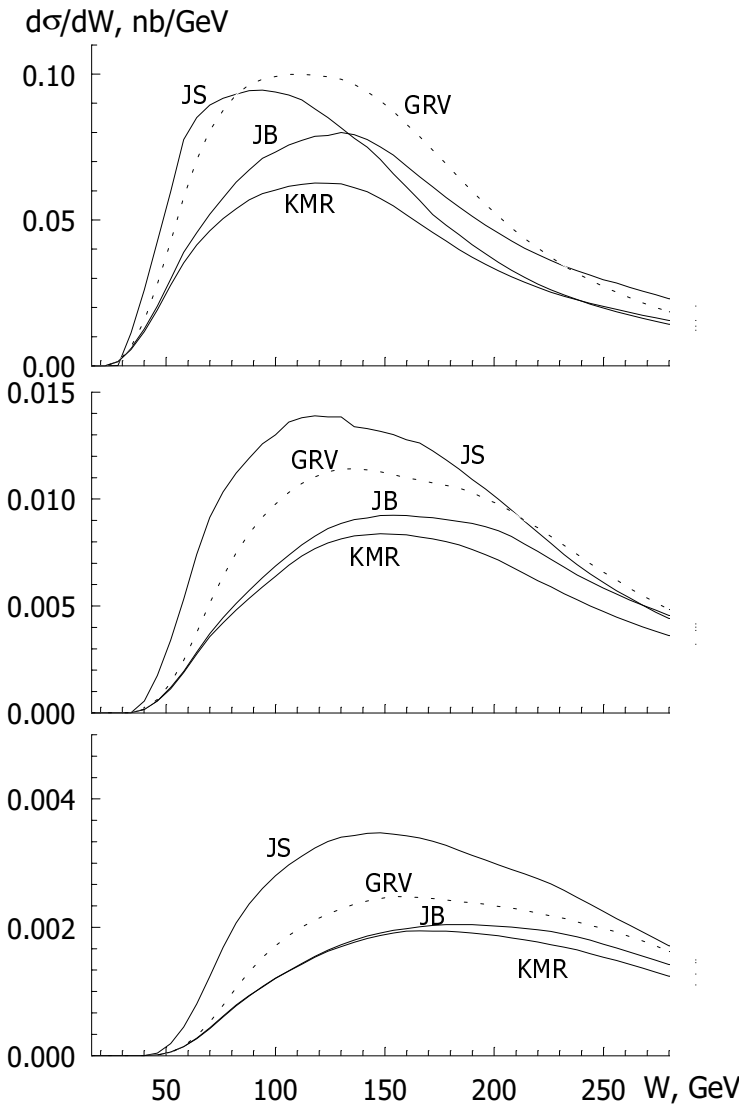


**Fig. 5.** The theoretical predictions for the  $W$ -spectra at the various cut on the  $D^*$  meson transverse momentum ( $p_T > 2, 4, 6$  GeV, correspondingly from up to down) and  $|\eta| < 1.5$ .

model and nonrelativistic approximation the production of the  $J/\psi$  meson is considered as the production of a quark-antiquark system in the color singlet state with orbital momentum  $L = 0$  and spin momentum  $S = 1$ . The binding energy and relative momentum of quarks in the  $J/\psi$  are neglected. In such a way  $M = 2m_c$  and  $p_c = p_{\bar{c}} = \frac{p}{2}$ , where  $p$  is the 4-momentum of the  $J/\psi$ ,  $p_c$  and

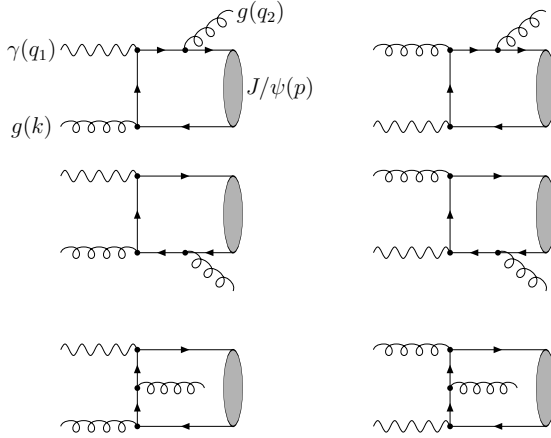


**Fig. 6.** Diagrams used for description partonic process  $\gamma + g \rightarrow J/\psi + g$ .

$p_{\bar{c}}$  are 4-momenta of quark and antiquark. Taking into account the formalism of the projection operator [28] the amplitude of the process  $\gamma g \rightarrow J/\psi g$  may be obtained from the amplitude of the process  $\gamma g \rightarrow \bar{c}cg$  after replacement:

$$V^i(p_{\bar{c}})\bar{U}^j(p_c) \rightarrow \frac{\Psi(0)}{2\sqrt{M}}\hat{\varepsilon}(p)(\hat{p} + M)\frac{\delta^{ij}}{\sqrt{3}}, \quad (15)$$

where  $\hat{\varepsilon}(p) = \varepsilon_\mu(p)\gamma^\mu$ ,  $\varepsilon_\mu(p)$  is a 4-vector of the  $J/\psi$  polarization,  $\frac{\delta^{ij}}{\sqrt{3}}$  is the color factor,  $\Psi(0)$  is the nonrelativistic meson wave function at the origin. The matrix elements of the process  $\gamma g^* \rightarrow J/\psi g$  may be presented as follows:

$$M_i = KC^{ab}\varepsilon_\alpha(q_1)\varepsilon_\mu^a(q)\varepsilon_\beta^b(q_2)\varepsilon_\nu(p)M_i^{\alpha\beta\mu\nu}, \quad (16)$$

$$M_1^{\alpha\beta\mu\nu} = \text{Tr} \left[ \gamma^\nu(\hat{p} + M)\gamma^\alpha \frac{\hat{p}_c - \hat{q}_1 + m_c}{(p_c - q_1)^2 - m_c^2} \gamma^\mu \frac{-\hat{p}_{\bar{c}} - \hat{q}_2 + m_c}{(p_{\bar{c}} + q_2)^2 - m_c^2} \gamma^\beta \right], \quad (17)$$

$$M_2^{\alpha\beta\mu\nu} = \text{Tr} \left[ \gamma^\nu(\hat{p} + M)\gamma^\beta \frac{\hat{p}_c + \hat{q}_2 + m_c}{(p_c + q_2)^2 - m_c^2} \gamma^\alpha \frac{\hat{k} - \hat{p}_{\bar{c}} + m_c}{(q - p_{\bar{c}})^2 - m_c^2} \gamma^\mu \right], \quad (18)$$

$$M_3^{\alpha\beta\mu\nu} = \text{Tr} \left[ \gamma^\nu(\hat{p} + M)\gamma^\alpha \frac{\hat{p}_c - \hat{q}_1 + m_c}{(p_c - q_1)^2 - m_c^2} \gamma^\beta \frac{\hat{k} - \hat{p}_{\bar{c}} + m_c}{(q - p_{\bar{c}})^2 - m_c^2} \gamma^\mu \right], \quad (19)$$

$$M_4^{\alpha\beta\mu\nu} = \text{Tr} \left[ \gamma^\nu(\hat{p} + M)\gamma^\mu \frac{\hat{p}_c - \hat{k} + m_c}{(p_c - q)^2 - m_c^2} \gamma^\alpha \frac{-\hat{p}_{\bar{c}} - \hat{q}_2 + m_c}{(q_2 + p_{\bar{c}})^2 - m_c^2} \gamma^\beta \right], \quad (20)$$

$$M_5^{\alpha\beta\mu\nu} = \text{Tr} \left[ \gamma^\nu(\hat{p} + M)\gamma^\beta \frac{\hat{p}_c + \hat{q}_2 + m_c}{(p_c + q_2)^2 - m_c^2} \gamma^\mu \frac{\hat{q}_1 - \hat{p}_{\bar{c}} + m_c}{(q_1 - p_{\bar{c}})^2 - m_c^2} \gamma^\alpha \right], \quad (21)$$

$$M_6^{\alpha\beta\mu\nu} = \text{Tr} \left[ \gamma^\nu (\hat{p} + M) \gamma^\mu \frac{\hat{p}_c - \hat{k} + m_c}{(p_c - q)^2 - m_c^2} \gamma^\beta \frac{\hat{q}_1 - \hat{p}_{\bar{c}} + m_c}{(q_1 - p_{\bar{c}})^2 - m_c^2} \gamma^\alpha \right], \quad (22)$$

where  $q_1$  is the 4-momentum of the photon,  $q$  is the 4-momentum of the initial gluon,  $q_2$  is the 4-momentum of the final gluon,

$$K = e_c e g_s^2 \frac{\Psi(0)}{2\sqrt{M}}, \quad C^{ab} = \frac{1}{\sqrt{3}} \text{Tr}[T^a T^b], \quad e_c = \frac{2}{3}, \quad e = \sqrt{4\pi\alpha}, \quad g_s = \sqrt{4\pi\alpha_s}.$$

The summation on the photon, the  $J/\psi$  meson and final gluon polarizations is carried out by covariant formulae:

$$\sum_{\text{spin}} \varepsilon_\alpha(q_1) \varepsilon_\beta(q_1) = -g_{\alpha\beta}, \quad (23)$$

$$\sum_{\text{spin}} \varepsilon_\alpha(q_2) \varepsilon_\beta(q_2) = -g_{\alpha\beta}, \quad (24)$$

$$\sum_{\text{spin}} \varepsilon_\mu(p) \varepsilon_\nu(p) = -g_{\mu\nu} + \frac{p_\mu p_\nu}{M^2}. \quad (25)$$

In case of the initial BFKL gluon we use the prescription (5). For studing  $J/\psi$  polarized photoproduction we introduce the 4-vector of the longitudinal polarization as follows:

$$\varepsilon_L^\mu(p) = \frac{p^\mu}{M} - \frac{M p_N^\mu}{(pp_N)}. \quad (26)$$

In the high energy limit of  $s = 2(q_1 p_N) \gg M^2$  the polarization 4-vector satisfies usual conditions  $(\varepsilon_L \varepsilon_L) = -1$ ,  $(\varepsilon_L p) = 0$ .

Traditionally for a description of charmonium photoproduction

processes the invariant variable  $z = (pp_N)/(q_1 p_N)$  is used. In the rest frame of the proton one has  $z = E_\psi/E_\gamma$ . In the  $k_T$ -factorization approach the differential on  $p_T$  and  $z$  cross section of the  $J/\psi$  photoproduction may be written as follows:

$$\frac{d\sigma(\gamma p \rightarrow J/\Psi X)}{dp_T^2 dz} = \frac{1}{z(1-z)} \int_0^{2\pi} \frac{d\varphi}{2\pi} \int_0^{\mu^2} d\mathbf{k}_T^2 \Phi(x, \mathbf{k}_T^2, \mu^2) \frac{\overline{|M|^2}}{16\pi(xs)^2}. \quad (27)$$

The analytical calculation of the  $\overline{|M|^2}$  is performed with help of REDUCE package and results are saved in the FORTRAN codes as a function of  $\hat{s} = (q_1 + q)^2$ ,  $\hat{t} = (p - q_1)^2$ ,  $\hat{u} = (p - q)^2$ ,  $\mathbf{p}_T^2$ ,  $\mathbf{k}_T^2$  and  $\cos(\varphi)$ . We directly have tested that

$$\lim_{\mathbf{k}_T^2 \rightarrow 0} \int_0^{2\pi} \frac{d\varphi}{2\pi} \overline{|M|^2} = \overline{|M_{PM}|^2}, \quad (28)$$

where  $\mathbf{p}_T^2 = \frac{\hat{t}\hat{u}}{\hat{s}}$  in the  $\overline{|M|^2}$  and  $\overline{|M_{PM}|^2}$  is the square of the amplitude in the conventional parton model [24]. In the limit of  $\mathbf{k}_T^2 = 0$  from formula (27) it is easy to find the differential cross section in the parton model, too:

$$\frac{d\sigma^{PM}(\gamma p \rightarrow J/\Psi X)}{dp_T^2 dz} = \frac{\overline{|M_{PM}|^2} x G(x, \mu^2)}{16\pi(xs)^2 z(1-z)}. \quad (29)$$

However, making calculations in the parton model we use formula (27), where integration over  $\mathbf{k}_T^2$  and  $\varphi$  is performed numerically, instead of (29). This method fixes the common normalization factor for both approaches and gives a direct opportunity to study effects connected with virtuality of the initial BFKL gluon in the partonic amplitude.

## 5 $J/\psi$ Photoproduction at HERA

After we fixed the selection of the gluon distribution functions  $G(x, \mu^2)$  or  $\Phi(x, \mathbf{k}_T^2, \mu^2)$  there are two parameters only, which values determine the common normalization factor of the cross section under consideration:  $\Psi(0)$  and  $m_c$ . The value of the  $J/\psi$  meson wave function at the origin may be calculated in a potential model or obtained from experimental well known decay width  $\Gamma(J/\psi \rightarrow \mu^+ \mu^-)$ . In our calculation we used the following choice  $|\Psi(0)|^2 = 0.064$  GeV<sup>3</sup> which corresponds to NRQCD coefficient  $\langle O^{J/\psi}, \mathbf{1}^3S_1 \rangle = 1.12$  GeV<sup>3</sup> as the same as in [26]. Note, that this value is a little smaller (30 %) than the value which was used in our paper [23]. Concerning a charmed quark mass, the situation is not clear up to the end. From one hand, in the nonrelativistic approximation one has  $m_c = \frac{M}{2}$ , but there are many examples of taking smaller value of a  $c$ -quark mass in the amplitude of a hard process, for example  $m_c = 1.4$  GeV. Taking into consideration above mentioned we perform calculations at  $m_c = 1.5$  GeV. The cinematic region under consideration is determined by the following conditions:  $Q^2 < 1$  GeV<sup>2</sup>,  $60 < W < 240$  GeV,  $0.3 < z < 0.9$  and  $p_T > 1$  GeV, which correspond to the H1 Collaboration data [29]. We assume that the contribution of the color octet mechanism is large at the  $z > 0.9$  only. In the region of the small values of the  $z < 0.2$  the contribution of the resolved photon processes [30] as well as the charm excitation processes [31] may be large, too. All of these contributions are not in our consideration.

Figures 7–10 show our results which were obtained as in the conventional parton model as well as in the  $k_T$ -factorization approach with the different parameterizations of the unintegrated gluon distribution function. The dependence of the results on selection of a hard scale parameter  $\mu$  is much less than the dependence on selection of a  $c$ -quark mass and selection of a parameterization. We put  $\mu^2 = M^2 + \mathbf{p}_T^2$  in a gluon distribution function and in a running constant  $\alpha_s(\mu^2)$ .

The count of a transverse momentum of the BFKL gluons in the  $k_T$ -factorization approach results in a flattening of the  $p_T$ -spectrum of the  $J/\psi$  as contrasted by predictions of the parton model. For the first time this effect was indicated in the [22], and later in [23]. Figure 7 shows the result of our calculation for the  $p_T$  spectrum of the  $J/\psi$  mesons. Using the  $k_T$ -factorization approach we have obtained the harder  $p_T$ -spectrum of the  $J/\psi$  than has been predicted in the LO parton model. It is visible that at large values of  $p_T$  only the  $k_T$ -factorization approach gives correct description of the data [29]. However, it is impossible to consider this visible effect as a direct indication on nontrivial developments of the small- $x$  physics. In the article [26] was shown that the calculation in the

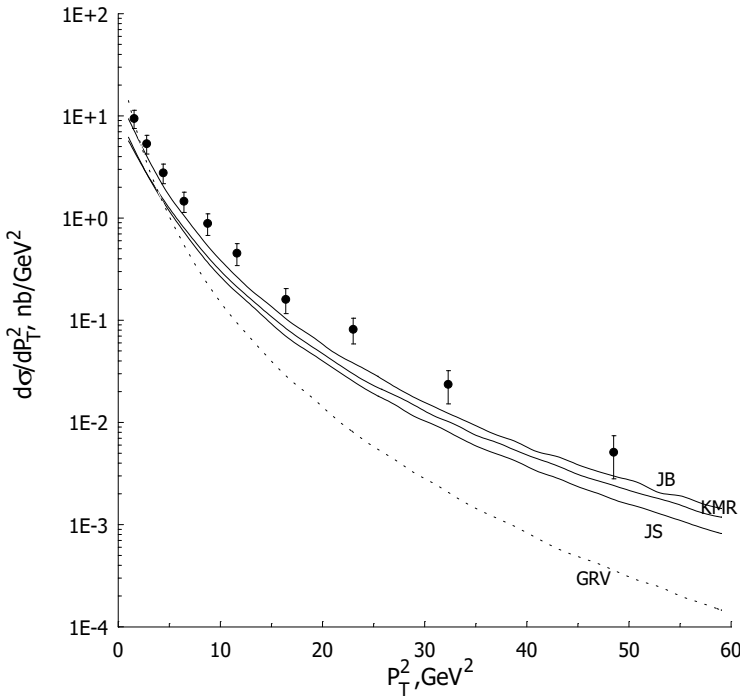


Fig. 7. The  $J/\psi$  spectrum on  $p_T^2$  at the  $60 < W < 240$  GeV and  $0.3 < z < 0.9$ .

NLO approximation gives a harder  $p_T$  spectrum of the  $J/\psi$  meson, too, which will agree with the data at the large  $p_T$ .

In the  $k_T$ -factorization approach JB parameterization [8] gives  $p_T$ -spectrum, which is very close to experimental data. From the another hand in the case of JS parameterization [9] the additional  $K$ -factor approximately equal 2 is needed.

The  $z$  spectra are shown in Fig. 8 at the various choice of the  $p_T$  cut:  $p_T > 2$ , 4 and 6 GeV, correspondingly. The relation between the theoretical predictions and experimental data is the same as in Fig. 7. The  $k_T$  factorization approach give more correct description of the data especially at large value of  $z$  where the curve obtained in the collinear parton model tends to zero.

Figure 9 shows the dependence of the total  $J/\psi$  photoproduction cross section on  $W$  at  $0.3 < z < 0.8$  and  $p_T > 1$  GeV. The shape of this dependence agrees well with the result obtained using JS parameterization [9] or KMR [10] parameterization. However, the predicted absolute value of the cross section  $\sigma_{\gamma p}$  is smaller by factor 2 than obtained data [29]. The results of calculation using JB [8] or GRV [7] parameterizations are larger and coincide with the data [29] better.

As it was mentioned above, the main difference between the  $k_T$ -factorization approach and the conventional parton model is nontrivial polarization of the BFKL gluon. It is obvious, that such a spin condition of the initial gluon should

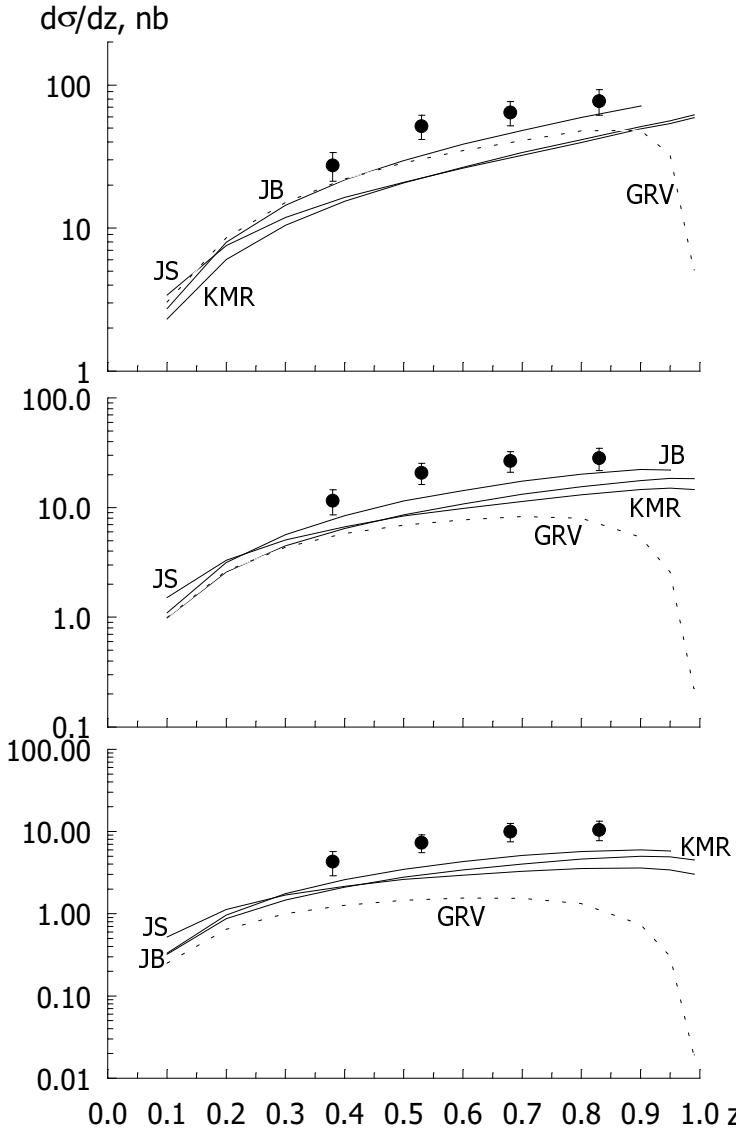


**Fig. 8.** The  $J/\psi$  spectrum on  $z$  at the  $60 < W < 240$  GeV ( $p_T > 1, 2, 3$  GeV, correspondingly from up to down).

result in observed spin effects during the birth of the polarized  $J/\psi$  meson. We have performed calculations for the spin parameter  $\alpha$  as a function  $z$  or  $p_T$  in the conventional parton model and in the  $k_T$ -factorization approach :

$$\alpha(z) = \frac{\frac{d\sigma_{tot}}{dz} - 3\frac{d\sigma_L}{dz}}{\frac{d\sigma_{tot}}{dz} + \frac{d\sigma_L}{dz}}, \quad \alpha(p_T) = \frac{\frac{d\sigma_{tot}}{dp_T} - 3\frac{d\sigma_L}{dp_T}}{\frac{d\sigma_{tot}}{dp_T} + \frac{d\sigma_L}{dp_T}} \quad (30)$$

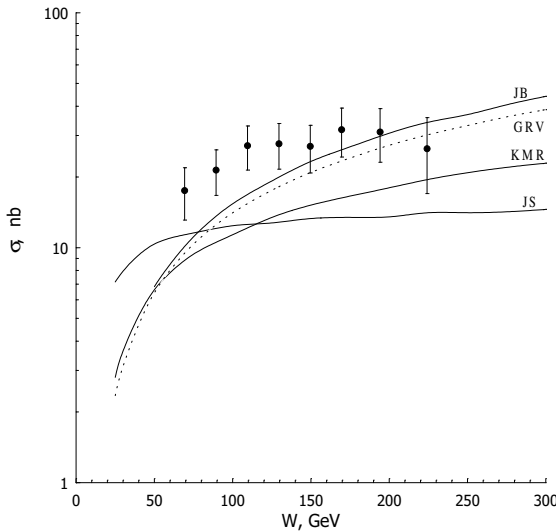


**Fig. 9.** The total  $J/\psi$  photoproduction cross section versus  $W$  at  $0.3 < z < 0.8$  and  $p_T > 1$  GeV.

Here  $\sigma_{tot} = \sigma_L + \sigma_T$  is the total  $J/\psi$  production cross section,  $\sigma_L$  is the production cross section for the longitudinal polarized  $J/\psi$  mesons,  $\sigma_T$  is the production cross section for the transverse polarized  $J/\psi$  mesons. The parameter  $\alpha$  controls the angle distribution for leptons in the decay  $J/\psi \rightarrow l^+l^-$  in the  $J/\psi$  meson rest frame:

$$\frac{d\Gamma}{d\cos(\theta)} \sim 1 + \alpha \cos^2(\theta). \quad (31)$$

The theoretical results for the parameter  $\alpha(z)$  are very close to each other irrespective of the choice of an approach or a gluon parameterization [23].

For the parameter  $\alpha(p_T)$  we have found strongly opposite predictions in the parton model and in the  $k_T$ -factorization approach, as it is visible in Fig. 10. The parton model predicts that  $J/\psi$  mesons should have transverse polarizations at the large  $p_T$  ( $\alpha(p_T) = 0.6$  at the  $p_T = 6$  GeV), but  $k_T$ -factorization approach predicts that  $J/\psi$  mesons should be longitudinally polarized ( $\alpha(p_T) = -0.4$  at the  $p_T = 6$  GeV). The experimental points lie in the range  $0 < p_T < 5$  GeV and they have the large errors. However, it is visible that  $\alpha(p_T)$  decrease as  $p_T$  changes from 1 to 5 GeV. This fact coincide with theoretical prediction obtained in the  $k_T$ -factorization approach. Nowadays, a result of the NLO parton model calculation in the case of the polarized  $J/\psi$  meson photoproduction is unknown. It should be an interesting subject of future investigations. If the count of the NLO corrections will not change predictions of the LO parton model for  $\alpha(p_T)$ , the experimental measurement of this spin effect will be a direct signal about BFKL gluon dynamics.

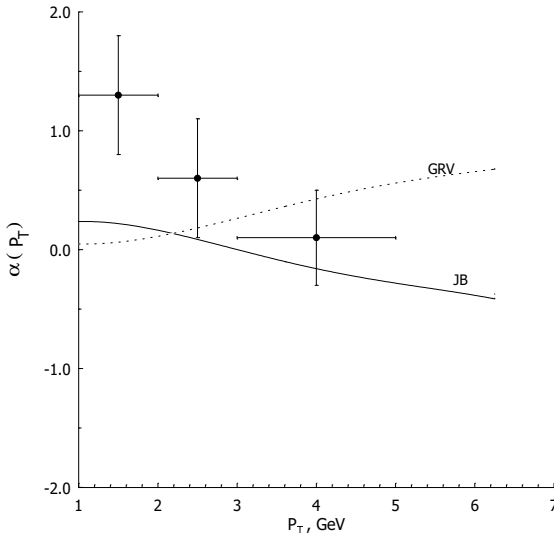


**Fig. 10.** Parameter  $\alpha$  as a function of  $p_T$  at  $0.3 < z < 0.9$ ,  $p_T > 1$  GeV,  $60 < W < 240$  GeV.

Nowadays, the experimental data on  $J/\Psi$  polarization in photoproduction at large  $p_T$  are absent. However there are similar data from CDF Collaboration [32], where  $J/\psi$  and  $\psi'$   $p_T$ -spectra and polarizations have been measured. Opposite the case of  $J/\psi$  photoproduction, the hadroproduction data needs to take into account the large color-octet contribution in order to explain  $J/\psi$  and  $\psi'$  production at Tevatron in the conventional collinear parton model. The relative weight of color-octet contribution may be smaller if we use  $k_T$ -factorization approach, as was shown recently in [33–36]. The predicted using collinear parton model transverse polarization of  $J/\psi$  at large  $p_T$  is not supported by the CDF data, which can be roughly explained by the  $k_T$ -factorization approach [34]. In conclusion, the number of theoretical uncertainties in the case of  $J/\psi$  meson hadroproduction is much more than in the case of photoproduction

and they need more complicated investigation, which is why the future experimental analysis of  $J/\psi$  photoproduction at THERA will be clean check of the collinear parton model and the  $k_T$ -factorization approach.

The authors would like to thank M. Ivanov and S. Nedelko for kind hospitality during workshop “Heavy quark - 2002” in Dubna, S. Baranov, A. Lipatov and O. Teryaev for discussions on the  $k_T$ -factorization approach of QCD and H. Jung for the valuable information on unintegrated gluon distribution functions. This work has been supported in part by the Russian Foundation for Basic Research under Grant 02-02-16253.

## References

1. G. Sterman et al.: Rev. Mod. Phys. **59**, 158 (1995)
2. V.N. Gribov and L.N. Lipatov: Sov. J. Nucl. Phys. **15**, 438 (1972) Yu.A. Dokshitser: Sov. Phys. JETP. **46**, 641 (1977) G. Altarelli and G. Parisi: Nucl. Phys. **B126**, 298 (1977)
3. L.V. Gribov, E.M. Levin, M.G. Ryskin: Phys. Rep. **100**, 1 (1983)
4. J.C. Collins and R.K. Ellis: Nucl. Phys. **360**, 3 (1991)
5. S. Catani, M. Ciafoloni and F. Hautmann: Nucl. Phys. **B366**, 135 (1991)
6. E. Kuraev, L. Lipatov, V. Fadin: Sov. Phys. JETP **44**, 443 (1976) Y. Balitskii and L. Lipatov: Sov. J. Nucl. Phys. **28**, 822 (1978)
7. M. Gluck, E. Reya and A. Vogt: Z. Phys. **C67**, 433 (1995)
8. J. Bluemlein: DESY 95-121.
9. H. Jung, G. Salam: Eur. Phys. J. **C19**, 351 (2001)
10. M.A. Kimber, A.D. Martin and M.G. Ryskin: Phys. Rev. **D63**, 114027 (2001)
11. J. Breitweg et al.[ZEUS Coll.]: Eur. Phys. J. **C6**, 67 (1999) Phys. Lett. **B481**, 213 (2000)
12. C. Adloff et al.[H1 Coll.]: Nucl. Phys. **B545**, 21 (1999)
13. C. Peterson et al.: Phys. Rev. **D27**, 105 (1983)
14. A.V. Berezhnoy, V.V. Kiselev and A.K. Likhoded: (hep-ph/9901333, hep-ph/9905555)
15. R. Akers et al.[OPAL Coll.]: Z. Phys. **C67**, 27 (1995)
16. P. Nason and C. Oleari: Phys. Lett. **B447**, 327 (1999)
17. B. Kniehe et al.: Z. Phys. **C76**, 689 (1997) J. Binnewicks et al.: Phys. Rev. **D58**, 014014 (1998)
18. V.A. Saleev and N.P. Zotov: Mod. Phys. Lett. **A11**, 25 (1996)
19. V.M. Budnev et al.: Phys. Rep. **15**, 181 (1974)
20. S. Frixione et al.: Phys. Lett. **B319**, 339 (1993)
21. S. Baranov, N. Zotov: Phys. Lett. **B458**, 389 (1999)
22. V.A. Saleev, N.P. Zotov: Mod. Phys. Lett. **A9**, 151; 1517 (1994)
23. V.A. Saleev: Phys. Rev. **D65**, 054041 (2002)
24. E.L. Berger and D. Jones: Phys. Rev. **D23**, 1521 (1981) R. Baier and R. Rückl: Phys. Lett. **B102**, 364 (1981) S.S. Gershtein, A.K. Likhoded, S.R. Slabospiskii: Sov. J. Nucl. Phys. **34**, 128 (1981)
25. G.T. Bodwin, E. Braaten, G.P. Lepage: Phys. Rev **D51**, 1125 (1995)
26. M. Kramer: Nucl. Phys. **B459**, 3 (1996)
27. Aid et al.[H1 Coll.]: Nucl. Phys. **B472**, 32 (1996) J. Breitweg et al.[ZEUS Coll.]: Z. Phys. **C76**, 599 (1997)
28. B. Guberina et al.: Nucl. Phys. **B174**, 317 (1980)
29. C. Adloff et al.[H1 Coll.]: DESY 02-059 (2002)
30. H. Jung, G.A. Schuler and J. Terron: DESY 92-028 (1992)
31. V.A. Saleev: Mod. Phys. Lett. **A9**, 1083 (1994)
32. T. Affolder et al.[CDF Coll.]: Phys. Rev. Lett. **85**, 2886 (2000)
33. F. Yuan, K-T. Chao: Phys. Rev. **D63**, 034006 (2001)
34. F. Yuan, K-T. Chao: Phys. Rev. Lett. **D87**, 022002-L (2001)
35. Ph. Hägler et al.: Phys. Rev. Lett. **86**, 1446 (2001)
36. Ph. Hägler et al.: Phys. Rev. **D63**, 077501 (2001)